

Exotic magnetic structures in ultrathin helimagnetic holmium films

F. Cinti, A. Cuccoli, and A. Rettori

CNISM and Department of Physics, University of Florence, 50019 Sesto Fiorentino (FI), Italy

(Received 16 June 2008; published 14 July 2008)

The problem of spin arrangement in ultrathin films of materials with competing medium-range interactions has been investigated by classical Monte Carlo simulations, assuming the model pertinent to bulk holmium. We find that in addition to distorted helical configurations at low temperature, unusual blocked phases—with some inner disordered planes intercalating ordered blocks and with the inner planes undergoing a Kosterlitz-Thouless phase transition as the temperature rises—may appear at intermediate temperature. The blocked phases turn out to be much more structured than those predicted by mean-field calculations, and their contribution to the static structure factor appear substantially indistinguishable from that corresponding to helical order thus constituting a challenge for their experimental probing by conventional elastic scattering techniques.

DOI: 10.1103/PhysRevB.78.020402

PACS number(s): 64.60.an, 64.60.De, 75.10.Hk, 75.40.Cx

The availability of sophisticated growth and characterization techniques has allowed us to investigate the thickness dependence of the critical temperature of magnetic ultrathin films.¹ Among them, particular interest was attracted by films of rare-earth metals, which are characterized by a helimagnetic (HM) order in bulk samples. Recent experimental work² showed that the critical behavior differs qualitatively with respect to that of transition metals where collinear order is commonly observed;¹ an interpretation of the experimental outcomes was until now attempted only on the basis of a mean-field theory,^{2,3} which in turn gave some unexpected peculiar behavior for the thinner films (as detailed below). By the Monte Carlo simulation (MCS) work reported in this letter, we aim at shedding some light on the behavior of thin films of spins with competitive middle-range interactions—looking at effects beyond the capability of the mean-field approximation.

When suitable corrections^{1,4} to the usual finite-size scaling (FSS) analysis are properly taken into account, the experimental results obtained for films displaying magnetic collinear order are consistent with the prediction by Fisher and co-workers.^{5,6}

$$[T_C(\infty) - T_C(n)]/T_C(\infty) = (C_0/n)^{-\lambda}, \quad (1)$$

$T_C(\infty)$ and $T_C(n)$ being the critical temperatures of the bulk material and of a film with n monolayers (ML), respectively, and with the shift exponent λ defined by the universality class of the bulk system. Much stronger effects are expected in films of materials with modulated long period magnetic ordering in the bulk. When the thickness is comparable with the periodicity of the ordered structure, we expect that even the magnetic arrangement itself can be strongly modified. Rare-earth helimagnets such as Ho, Dy, and Tb (Ref. 7) represent the best candidates to put into evidence such finite-size effects. In such compounds, the long period of the ordered structure is due to the competitive interactions having different ranges and the presence of two surfaces can have dramatic consequences. Bulk Ho crystallizes in a hexagonal-close-packed (hcp) lattice. For $T < T_N = 132$ K it exhibits ferromagnetically ordered (ab) basal planes and HM order along the c direction.⁷ The most accurate localized spin effective exchange model requires the inclusion of interactions

extending up to the sixth nearest-neighbor (NN) plane.^{7,8} An interesting experimental study on ultrathin films ($n = 11-89$ ML) of Ho was performed by Weschke *et al.*² By neutron diffraction and resonant soft X-ray, they measured the static structure factor $S(\vec{q})$: a well defined peak at wave vector $\vec{q} = (0, 0, \tau)$, with $\tau = 0.33 \text{ \AA}^{-1}$, was found for every thickness n ; such feature was interpreted² as the signature of the presence of a HM order in the full range $n = 11-89$ ML (Ref. 2), below an n -dependent temperature $T_N(n)$. Weschke *et al.*² estimated the values of T_N and showed that its n dependence is well reproduced by the relation:⁹

$$[T_N(\infty) - T_N(n)]/T_N(n) = C'(n - n_0)^{-\lambda'}, \quad (2)$$

with $\lambda' = 0.70(7)$ and $n_0 = 10.8(5)$ ML, which is of the same order of the bulk helix wavelength. Weschke *et al.*² present also mean-field (MF) calculation (for details see Ref. 3) obtaining some unexpected results. The (n, T) phase diagram is characterized by two lines, denoted as $T_N(n)$ and $T_C(n)$, well reproduced by Eqs. (1) and (2), respectively.^{2,3} For $T < T_N$ films present a helix, which is more and more distorted when n decreases, with a limiting value n_0^{MF} qualitatively in agreement with Eq. (2). For $T > T_C$ the system is in the paramagnetic phase, while for $T_N < T < T_C$ and $n > n_0^{\text{MF}}$ a blocked phase (BP) is found with ferromagnetically ordered blocks (each one composed of 3–5 neighboring layers) having an alternating magnetic orientation. A curious result was obtained for $n = 7$: the central layer is in a paramagnetic state, in between still ordered subsystems.³

This MCS has a double aim: (i) Resolve to what extent, the thermal fluctuations, which in reduced dimensionality systems can be very important, affect and possibly modify the predictions of the MF treatment; (ii) Better clarify what information are reliably achievable from the measure of the static structure factor $S(q)$ in ultrathin films: an analysis of the MF results suggests indeed, as we will show below, that the presence of a peak in $S(q)$ at $\vec{q} \neq 0$ cannot be considered by itself an unambiguous evidence of a HM phase due to the intrinsic broadness of the peaks implied by the thinness of films.

We consider a slab of material built up with n monolayers

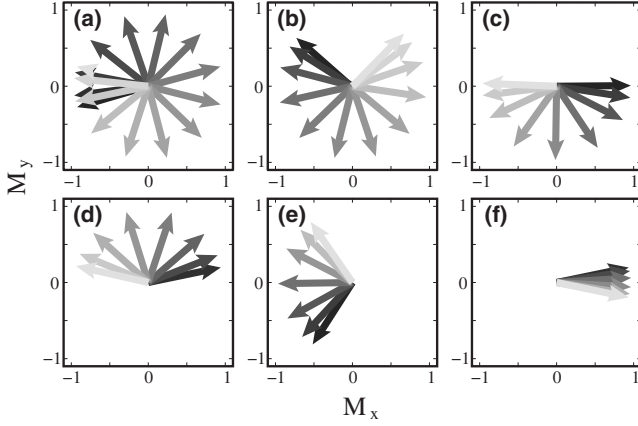


FIG. 1. Layer's magnetization vector profile at $T=10$ K for layer side length $L=80$ and different film thickness n : (a) $n=16$; (b) $n=12$; (c) $n=9$; (d) $n=8$; (e) $n=7$; and (f) $n=6$. Grayness saturation refers to layer index, the darkest arrow refers to the lower plane, and the lightest one refers to the upper plane of the film.

of spins properly stacked to form a hcp lattice: in each layer, representing the xy (ab) basal plane of Ho films, we arrange $L \times L$ spins. Periodic boundary conditions are adopted, while open boundary conditions are taken along the z (c) direction. We assume the Hamiltonian,⁸

$$H = -s(s+1) \sum_{i,j} J_{ij} \vec{S}_i \cdot \vec{S}_j + s^2 D \sum_{i=1} (S_i^z)^2, \quad (3)$$

with $|\vec{S}|=1$ and $s=8$. $D=0.25$ K is an easy-plane anisotropy,⁷ $J_{ij}=J_0=0.773$ K (Ref. 10), if i and j are nearest-neighbor spins on the same layer. While in the z direction, we take the six-constant model given by Bohr *et al.*⁸

MCS were carried out applying a judicious mix of Metropolis and over-relaxed moves¹² in order to reduce correlations among sampled configurations: usually one “MC step” is composed by one Metropolis and four/five over-relaxed moves per particle. For any run, up to 5×10^4 , initial MC steps are discarded in order to reach thermalization. Moreover at least three independent simulation runs are done for each T . Close to $T_N(n)$ the multiple-histogram method¹² is used, exploiting all the energy accumulated for each simulation; statistical errors are estimated by bootstrap-resampling data sets.¹² The spin arrangement as the film thickness decreases is shown in Fig. 1 where the single-layer magnetization vector is reported in the range $n=6-16$ for $L=80$ and at $T=10$ K. From the substantially helicoidal structure observed for $n=16$ (a quasibulk behavior), we move to a fan-like arrangement—with an increasing distortion of the helix at the boundary planes—as n is lowered until, for $n=6$, we get an almost collinear configuration. To investigate the role of the thermal fluctuations as T approaches the critical value, the T dependence of the Binder cumulants relative to layer magnetizations are reported for $n=16$ in Fig. 2(a). The (5, 6) [and symmetrically (11, 12)] planes lose their order at a lower temperature, $T=117.8(2)$ K, than the others [i.e., at $T=120.1(4)$ K]. We thus have a BP where blocks of consecutive planes, i.e., (1–4), (7–10), and (13–16), are ordered, while planes (5, 6) and (11, 12) are paramagnetic. In Fig.

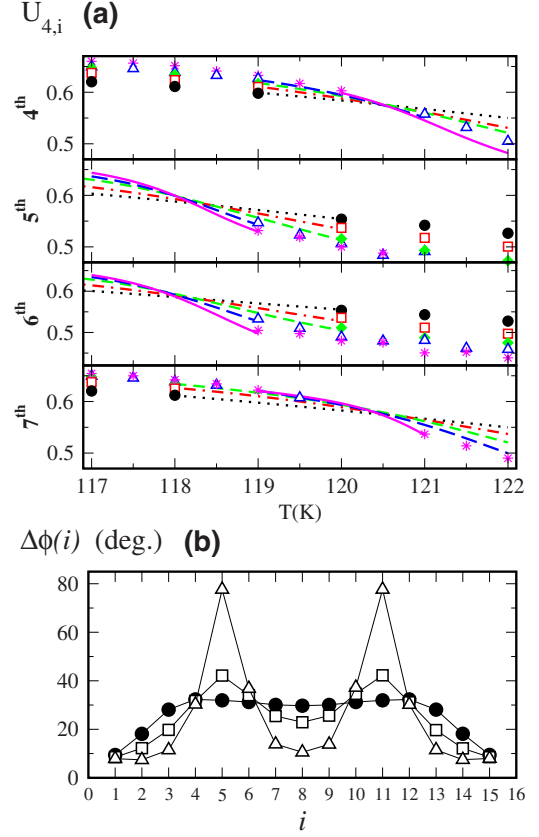


FIG. 2. (Color online) (a) Binder cumulant for the fourth, fifth, sixth, and seventh plane for the film thickness $n=16$. $L=16$ (filled circles), 24 (open squares), 32 (filled diamonds), 40 (open up triangles), and 48 (stars). (b) Phase angle $\Delta\phi(i) = \phi_{i+1} - \phi_i$ between magnetic moments for NN layers ($i+1, i$) for thickness $n=16$ and $L=48$ at $T=10$ (filled circles), 117 (open squares), and 120 K (open up triangles), respectively. Error bars included in the point.

2(b) the profile of the rotation angles between neighboring planes for $n=16$ at different T is plotted.¹³ Increasing T , the angles between the plane magnetizations in each block decrease, while the angles between different blocks increase. When $T > T_N(n)$ these latter angles approach 180° and consequently in the BP, we have a structure that can be represented as $\uparrow\uparrow\uparrow\uparrow\circ\circ\downarrow\downarrow\downarrow\downarrow\circ\circ\uparrow\uparrow\uparrow\uparrow$. The antiferromagnetic (AF) alignment of subsequent ordered blocks reveals their effective AF interaction resulting from medium-range inter-plane exchange coupling; similar behavior is observed for $n=12$ and 9. These results confirm and extend the MF predictions.^{2,3}

Surely, it is the phase transition of the planes disordering at lower temperatures that rules the overall sample transition from/to the HM structure. This is confirmed when properties as chirality $\kappa = \frac{1}{3(n-1)L^2 \sin Q_z} \sum_{il} (\vec{S}_{i,l} \times \vec{S}_{i+1,l})^z$ (where i labels the plane, l denotes the lattice site spin in the plane, and Q_z is the bulk Ho helical pitch), and related quantities are investigated. In Fig. 3(a) the chiral susceptibility, $\chi_\kappa = N\beta(\langle \kappa^2 \rangle - \langle \kappa \rangle^2)$, for $n=16$ is shown vs T for different L . A narrow peak is evident for $T=118.32(5)$ K, very near to the T values where the Binder cumulant for five and six (11 and 12) intersect. An estimate of the critical temperature for the onset

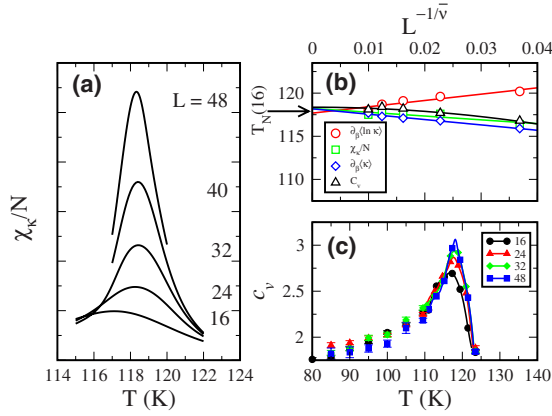


FIG. 3. (Color online) (a) χ_{κ} for $n=16$ and $L=48, 40, 32, 24$, and 16 . The greatest final relative errors is 0.2% for $L=48$ at maximum. (b) $T_N(16)$ plotted vs $1/L^{1/\bar{\nu}}$ obtained by FSS extrapolation of the four observables with $\bar{\nu}$ fit parameter. (c) Specific heat.

of HM order, $T_N(16)=117.9(2)\text{K}$, is obtained by FSS extrapolations of χ_{κ} , $\partial_{\beta}\langle\kappa\rangle$, $\partial_{\beta}\langle\ln\kappa\rangle$, and of the specific heat c_{ν} [Fig. 3(b)]. While such behavior could be expected—being the chiral order parameter strictly connected with the HM order—the analysis of an overall quantity as the specific heat may add substantial independent information. FSS extrapolation [Fig. 3(b)] of the maximum location of the specific heat [Fig. 3(c)] gives a value of $T_N(16)$ similar to that obtained by analyzing the quantities related to the chiral order parameter. A similar behavior is shown by films with $n=12$ and 9 , now being the central planes (the sixth and seventh one for $n=12$ and the fifth one for $n=9$) for those ordering at a lower T ; for $n=12$, using the same notation adopted in Ref. 2, we have the largest separation (~ 6 K) between $T_C(12)=119.8(3)\text{K}$ and $T_N(12)=113.6(1)\text{K}$.

A different perspective of the behavior of the film is obtained by looking at the order parameter $M = \frac{1}{n} \sum_{i=1}^n |\vec{M}_i|$, where \vec{M}_i is the magnetization vector for each plane i . M turns out to be relevant both in the HM phase and in the BP. This is apparent looking at its related quantities as the susceptibility χ_M [Fig. 4(a) for $n=12$]. Two anomalies are present for $T=114.1(2)\text{K}$ and $T=120.3(1)\text{K}$ [i.e., at a temperature T which roughly corresponds to $T_N(12)$ and $T_C(12)$, respectively]. An accurate analysis of χ_M shows that the origin of both $T_C(12)$ and of the BP are not to be searched in the finite-size dimension L of the samples here considered. In fact, at $T=114.1$ K ($\geq T_N(12)$), i.e., where the BP appears) a nonuniform field distribution is observed among different layers. In Fig. 4(b) the module of $\vec{H}_{\text{loc}}(i)$ is plotted. It is clear that, in the BP regime, the sixth and seventh planes are subject to a local field, which is smaller with respect to the bulk ones. Such planes thus behave as being decoupled from the others, displaying typical two-dimensional (2D) properties: the FSS analysis of $\chi_{M_{6,7}}$ ($\chi \propto L^{\gamma/\nu}$, where γ and ν are the critical exponents of the susceptibility and correlation length, respectively) gives an almost perfect Kosterlitz-Thouless (KT) trend¹⁴ with $\gamma/\nu=1.75(3)$ [see Fig. 4(c)]. At the same time, surprisingly enough, the scaling procedure on χ_M at $T_C(12)$ follows instead a XY three-dimensional (3D)-like behavior with $\gamma/\nu=1.96(2)$ [see Fig. 4(c)], which turns out to

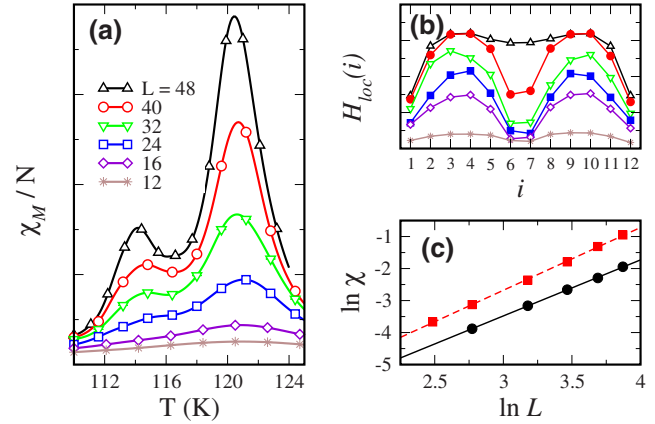


FIG. 4. (Color online) Thickness $n=12$: (a) Susceptibility χ_M (see text). (b) $|\vec{H}_{\text{loc}}(i)|$ vs plane index i in the BP: $T=112$ K (open up triangles), 114 K (filled circles), 116 K (open down triangles), 118 K (filled squares), 120 K (open diamonds), and 122 K (stars). (c) $\ln \chi_M$ (squares) and $\ln \chi_{M_{6,7}}$ (circles) maximum vs $\ln L$ (see text). The error bars are included in the symbols.

be in good agreement with previous theoretical results.¹⁴ We can thus sensibly speculate a global 3D structure composed by the ten slabs, 1–5 and 8–12, at $T_N(12) < T \leq T_C(12)$.

Regarding the possibility to discriminate between HM and BP structures in ultrathin films on the basis of the sole static structure factor, in Fig. 5 we report $S(\vec{q})$ vs $\vec{q}=(0,0,q_z)$ for $n=16$ in a large range of T , both below and above T_N : Apart from an obvious progressive intensity reduction by increasing T , we see that the peak shape and position remain unchanged. In order to confirm that for such ultrathin films the peak reflects only the overall structure periodicity, in Fig. 5 we report also the Fourier transform of the blocked structure $\uparrow\uparrow\uparrow\uparrow\circ\circ\downarrow\downarrow\downarrow\downarrow\circ\circ\uparrow\uparrow\uparrow\uparrow$ with saturated magnetization for each ferromagnetic plane (dashed line). Comparing it with $S(\vec{q})$ at $T=10$ K obtained by MCS, we see that the two curves are very similar with the same

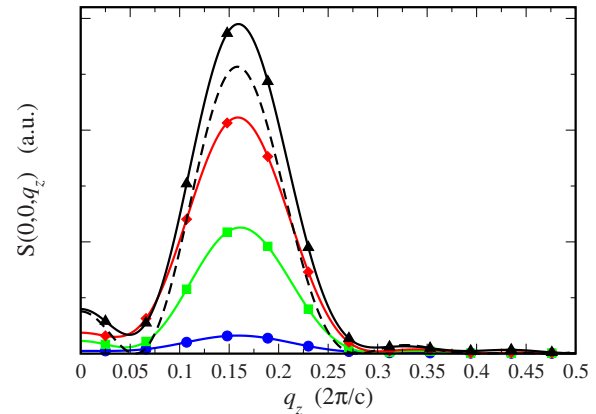


FIG. 5. (Color online) $S(\vec{q})$ vs $\vec{q}=(0,0,q_z)$ for thickness $n=16$ and $L=48$ at $T=10$ (black line, triangles), 116 (red line, diamonds), 119 (green line, squares), and 123 K (blue line, circle). Dashed black line: $S(\vec{q})$ of the block structure $\uparrow\uparrow\uparrow\uparrow\circ\circ\downarrow\downarrow\downarrow\downarrow\circ\circ\uparrow\uparrow\uparrow\uparrow$. Both the black curve ($T=10$ K) and the dashed one have been divided by a factor equal to six.

peak position and width and also with comparable intensities. We are lead to conclude that the HM phase and BP are indistinguishable from the viewpoint of the $S(\vec{q})$ alone.

The thickness $n=8$ is the borderline between helical/blocked regions and substantially ferromagnetic one. We find that at low T $S(\vec{q})$ presents a peak at $q_z=0.15$ but also with a very strong contribution at $q_z=0$. This peak recalls a fan structure (see also Fig. 1). Increasing T , the value of q_z , for which we have the maximum of $S(\vec{q})$, decreases and we do not have a BP but a smooth transition to the ferromagnetic order. Furthermore, FSS seems to suggest a KT trend for all planes at $T=110.6(3)$ K. Consequently, we are not able to discriminate between Eqs. (1) and (2) for the n dependence of the critical temperatures.

In conclusion, we have shown that in HM ultrathin films

the finite-size effects are much stronger than in ferromagnetic ones. Increasing T , the films show a phase transition from disordered HM order to a BP with some inner planes in the paramagnetic phase. Concerning the interpretation of experimental data on Ho, we point out that HM phase and BP in such ultrathin films cannot be discriminated by $S(\vec{q})$ measurements only. A possible experimental check of the observed phenomenology could be obtained by inelastic scattering measurements, which could reveal an increase in the fluctuations at the disordering of the inner planes.¹⁵

We are very grateful to H. Zabel for the useful correspondence, suggestions, and criticism. A.C. thanks D. A. Tennant for the useful discussions.

-
- ¹R. Zhang and R. F. Willis, Phys. Rev. Lett. **86**, 2665 (2001), and references therein.
- ²E. Weschke, H. Ott, E. Schierle, C. Schüssler-Langeheine, D. V. Vyalikh, G. Kaindl, V. Leiner, M. Ay, T. Schmitte, H. Zabel, and P. J. Jensen, Phys. Rev. Lett. **93**, 157204 (2004).
- ³P. J. Jensen and K. H. Bennemann, Surf. Sci. Rep. **61**, 129 (2006).
- ⁴M. Henkel, S. Andrieu, P. Bauer, and M. Piecuch, Phys. Rev. Lett. **80**, 4783 (1998).
- ⁵M. E. Fisher and M. N. Barber, Phys. Rev. Lett. **28**, 1516 (1972).
- ⁶M. N. Barber, in *Phase Transition and Critical Phenomena*, edited by C. Domb and J. Lebowitz (Academic, New York, 1983), Vol. 8, Chap. 2.
- ⁷J. Jensen and A. R. Mackintosh, *Rare Earth Magnetism (Structure and Excitations)* (Clarendon, Oxford, 1991) Also an in-plane hexagonal anisotropy is present but it becomes negligible for high T .
- ⁸J. Bohr, D. Gibbs, J. D. Axe, D. E. Moncton, K. L. D'amico, C. F. Majkrzak, J. Kwo, M. Hong, C. L. Chien, and J. Jensen, Physica B **159**, 93 (1989); The Hamiltonian (3) was used by C. C. Larsen, J. Jensen, and A. R. Mackintosh, Phys. Rev. Lett. **59**, 712 (1987) in order to study the spin waves in Ho.
- ⁹This relation was observed when Cr is interlayered in Fe/Cr superlattices: E. E. Fullerton, S. D. Bader, and J. L. Robertson, Phys. Rev. Lett. **77**, 1382 (1996).
- ¹⁰An experimental set of J_0 is lacking, we use $zJ_0=400 \mu\text{eV}$ ($z=6$), obtaining $T_N=124$ K for a bulk samples. We did not attempt any further adjustment of J_0 , as a quantitative prediction of experimental data is beyond the aim of this work, given that the assumed Hamiltonian is pertinent to the bulk, while in ultrathin films the strains, roughness can modify either in the RKKY interaction and/or in the anisotropy terms (Ref. 11).
- ¹¹L. Benito, M. Ciria, A. Fraile, D. Fort, J. S. Abell, and J. I. Arnaudas, Phys. Rev. Lett. **98**, 267201 (2007).
- ¹²D. P. Landau and K. Binder, *A Guide to Monte Carlo Simulation in Statistical Physics* (Cambridge University Press, Cambridge, 2000); M. E. Newman and G. T. Barkema, *Monte Carlo Methods in Statistical Physics* (Clarendon, Oxford, 1999).
- ¹³At $T=120$ K, i.e. above T_N , $\Delta\phi(i)$ for $i=4,5,6$ (and their symmetrical ones) can be obtained from MCS only thanks to the residual magnetisation of the inner planes due to finite-size effects; in the thermodynamic limit $\Delta\phi(4,5,6)$ becomes undefined, but $\phi(7)-\phi(4)$ is always well defined and approaches 180° .
- ¹⁴W. Janke and K. Nather, Phys. Rev. B **48**, 15807 (1993).
- ¹⁵H. Zabel (private communication).